The effect of shear and compressive strain on the low temperature crystallization of natural rubber

A. Stevenson
Malaysian Rubber Producers Research Association, Brickendonbury, Hertford, Herts SG13 8NL, UK
(Received 14 October 1985; revised 29 January 1986)

The kinetics of crystallization in rubber at low temperatures is studied macroscopically by means of small strain modulus measurements. This technique is very sensitive to small changes in crystallinity and is used to characterize the induction period, growth rate and equilibrium semi-crystalline state for rubber with various constant pre-strains. The effect of pre-strain in simple shear between 20% and 400% is described, as well as the effect of compressive pre-strain between 10% and 70%. A single empirical relationship is discovered between the Avrami growth rate exponent and a parameter characterizing pre-strain for shear, compressive and tensile modes of deformation and for all temperatures.

(Keywords: crystallization; rubber; strain; shear; compression; low temperature)

INTRODUCTION

The morphological aspects of crystallization in polymers have received considerable attention in the literature[1-4]. Less attention has been given to the kinetics of macroscopic changes in mechanical properties caused by crystallization, particularly in elastomers. It has been shown[5,6] that crystallization in natural rubber causes a volume decrease, relaxation in stress and an increase in Young's modulus[7] which can be as high as a factor of 200. The size of the modulus change makes it particularly sensitive to small changes in crystallinity. Moreover, modulus changes in rubber are of direct practical importance for rubber engineering components which may be exposed to low environmental temperatures[8]. The investigation reported here has thus aimed to study the macroscopic kinetics of crystallization in rubber by monitoring changes in Young's modulus.

Both the kinetics and morphology of crystallization generally depend on temperature and on strain orientation in the amorphous material. A previous publication[9] has reported on the effect of tensile strains on low temperature crystallization in a lightly vulcanized natural rubber, chosen as a model material. The present paper extends this to consider the effect of shear and compressive modes of deformation. An attempt is made to define a unified empirical expression to describe the crystallization kinetics for all three modes of deformation.

The stages of the crystallization process are characterized by three parameters: (i) an initial induction period, or time lag when no modulus change is detected, (ii) crystallization growth rates and (iii) an equilibrium modulus for the final semi-crystalline state. It was found previously[9] that induction period increased with decreasing tensile strain and exhibited a broad minimum with decreasing temperature between $-20°C$ and $-30°C$. The growth phase of crystallization was successfully described by the mathematical formalism of Avrami rate theory[10]. Experimental evidence did not however support the usual simple geometrical interpretation of the Avrami exponent, n. An empirical relation was discovered between n and the rubber extension ratio λ, while n was found to be independent of temperature. The equilibrium extent of crystallinity (about 30% for NR) was qualitatively in agreement with the thermodynamic theory of Flory[11]. The results for crystallization with shear and compressive strains in the rubber are also discussed in these terms. The three dimensional nature of the strain field for the compression case prohibits the usual thin film methods of observing crystal structures. For this case, test pieces have been 'freeze-fractured' after crystallization and examined by electron microscopy to provide some indirect evidence for crystalline morphologies. These observations are discussed in the light of the measured changes in compression modulus at low temperatures.

EXPERIMENTAL

Three different types of test piece were utilized in these experiments. The shear test pieces consisted of four rectangular parallelapipeds of rubber of dimensions 12 mm × 20 mm × 2 mm, bonded to outer steel plates and inner T-pieces in the configuration shown in *Figure 1a*. Pulling the T-pieces apart in the direction shown causes each of the four rubber slabs to deform in simple shear. The compression test pieces were circular discs of rubber of dimensions 13 mm diameter × 6 mm bonded to thin outer steel plates of the same diameter, as shown in *Figure 1b*. They were compressed uniaxially as illustrated causing rubber to bulge at the periphery according to an approximately parabolic profile. The tensile test pieces are shown in *Figure 1c* and were cut from rubber sheet to gauge length dimensions 2 mm × 2 mm × 25 mm.

A model natural rubber vulcanizate containing 100 parts SMR-CV60 to 1 part dicumyl peroxide, was used for all tests described in this paper. The test pieces were

0032-3861/86/081211-08$03.00

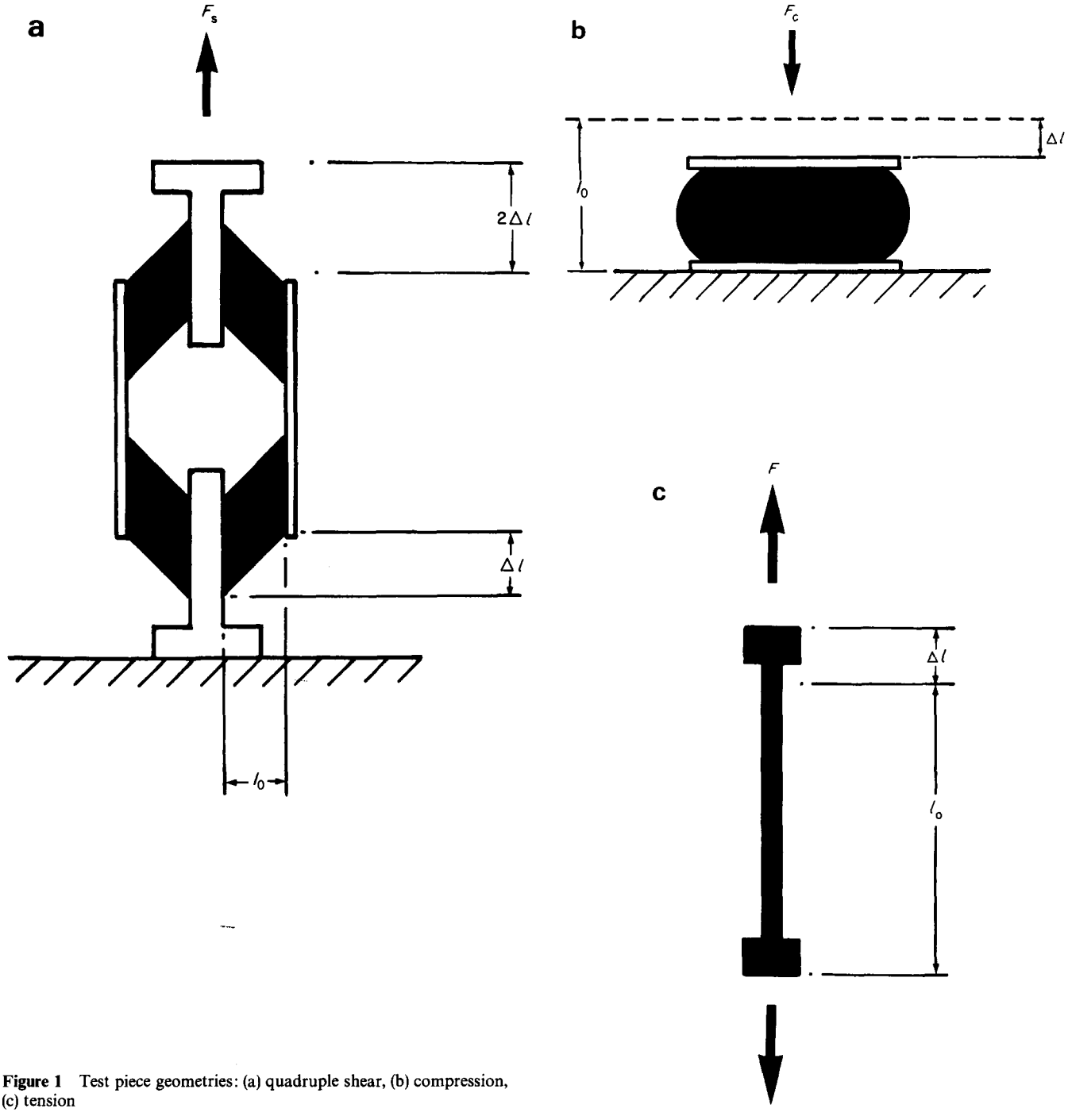

Figure 1 Test piece geometries: (a) quadruple shear, (b) compression, (c) tension

compression moulded by curing for 10 min at 100°C (to aid flow in the compression mould without crosslinking) followed by 60 min at 160°C. This produced a translucent rubber with C–C crosslinks and initial Young's modulus of 0.8 N/mm^2. This vulcanizate was chosen for its very rapid rate and extent of crystallization compared to normal engineering NR vulcanizates.

The test pieces were mounted in especially designed and constructed apparatus which enabled the force/deflection behaviour of each type of test piece to be determined inside a temperature cabinet at low temperatures. The test apparatus essentially consists of a simple miniaturized test machine with facilities for measuring force and displacement without removing the test piece from the low temperature chamber.

The basic experiment consisted in first applying a constant pre-strain to the test piece while the latter was at room temperature, then immersing in the low temperature cabinet and superimposing small strain cycles of 0–5%, each at a rate of 0.5 Hz and at sufficiently frequent intervals to characterize crystallization. From these strain cycles measurements were made of the differential force δF and differential displacement δl. The incremental elastic modulus E was then defined as:

$$E = \frac{\delta F / A_t}{\delta l / l_0} \tag{1}$$

where A_t is the true area of cross-secton in the initial pre-

strained state and l_0 is the initial test piece length (tension) or thickness (shear and compression).

All test pieces were annealed for 2 h at 90°C, 24 h before the start of each experiment. As described previously[9], this procedure was found to improve reproducibility of the results. The constant, static strain was applied while the test piece was at room temperature to avoid the nucleation or growth of any crystallites at low temperature that would not be characteristic of the test strain. Both the morphology and kinetics of crystallization are known to be affected by strain and this procedure aims to avoid the growth of 'mixed' morphologies.

RESULTS

Crystallization in compression

Deformation in compression. In general, modulus increases were observed for the low temperature crystallization of rubber discs in compression (*Figure 1b*) which were similar in character to those reported previously for thin rubber strips in tension (*Figure 1c*), insofar as they followed a sigmoidal increase to a quasi-equilibrium at higher moduli. *Figure 2* shows typical results for modulus changes resulting from crystallization at -40°C with compressive strains between 10% and 70%. In compression however (unlike shear or tension) the elastic modulus is strongly influenced by the shape of the test piece. It has been shown[11] that for a circular bonded disc of rubber:

$$E_c = E_0(1 + 2S^2) \tag{2}$$

where E_0 is Young's modulus and S is a shape factor defined as $D/2l$.

When a bonded rubber disc is compressed to high strains (such as 70%) the overall stress/strain curve is non-linear. If small-strain cycles are superimposed upon a constant strain level to determine the incremental elastic modulus defined in equation (1), then the effective shape factor for the small-strain cycles is increased—resulting in large modulus increases. In the limit, the incremental compression modulus will tend towards the bulk modulus of the material (~2000 MPa for 'unfilled natural rubber); this is three orders of magnitude greater than the Young modulus. It is a feature of the deformation of rubber in compression that rubber towards the outer free surface tends to deform in shear, while rubber at the centre of the disc tends to experience essentially hydrostatic pressure, where the higher bulk modulus applies. The compression modulus of the whole disc therefore consists of a mixture of bulk compression and a shear strain distribution; with tensile strains at the outer surface.

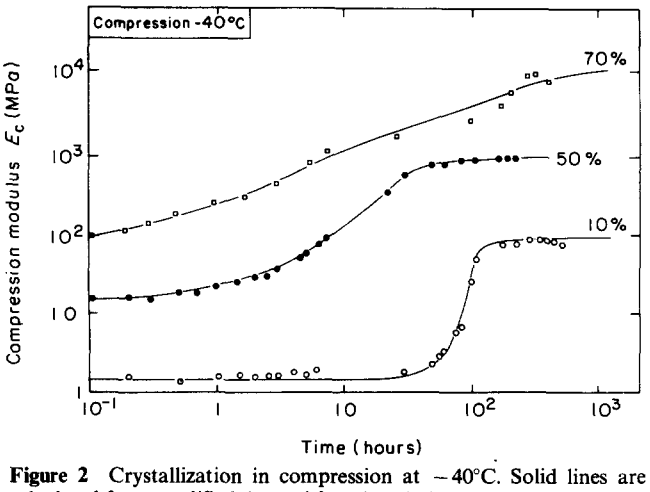

Figure 2 Crystallization in compression at −40°C. Solid lines are calculated from modified Avrami function, (○) 10% compression, (●) 50% compression, (□) 70% compression

Nucleation. In compression the initial elastic modulus depends strongly on the constant pre-strain level applied. This explains the different starting points for the incremental compression moduli in *Figure 2*. The other obvious effect of increasing applied strain is to decrease the time-lag before the onset of a measurable modulus change. This time-lag, defined here as the nucleation period, τ, for the development of embryo crystallites, is shown in *Figure 3* plotted against the extension ratio λ_c ($=1-\delta l/l$) for crystallization temperatures of −25°C and −40°C. The relationship depicted there is (within experimental uncertainty) in accord with the simple model introduced previously[9], whereby:

$$\tau(\lambda) - \tau_0 \exp(\beta\lambda) \tag{3}$$

where τ_0 is the induction period at zero strain ($\lambda = 1$) and* β

$$\beta = -5/2 \text{ for } \lambda > 1$$
$$= +5/2 \text{ for } \lambda < 1$$

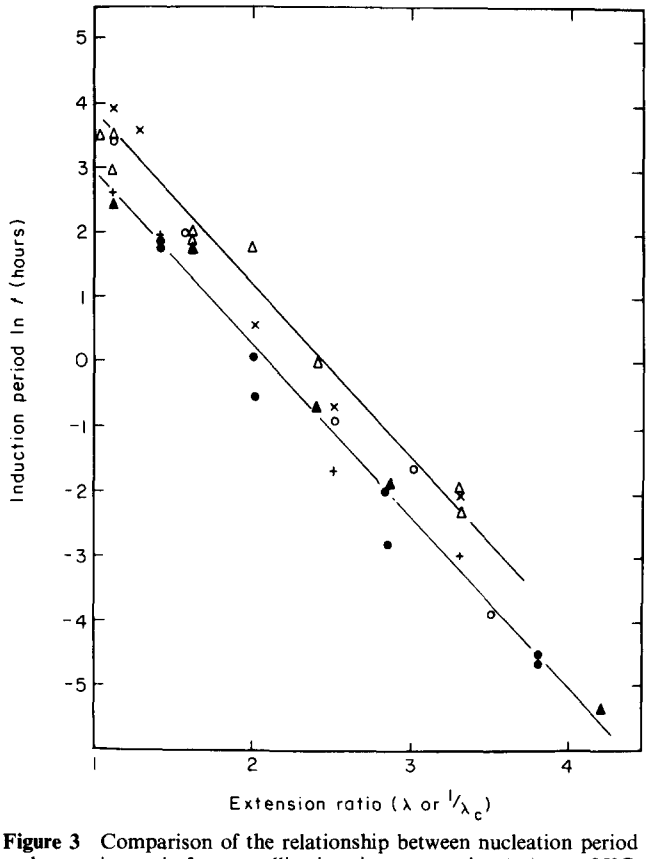

Figure 3 Comparison of the relationship between nucleation period and extension ratio for crystallization: in compression (+) at −25°C, (×) at −40°C; in tension (●) at −25°C, (○) at −40°C; in shear (▲) at −25°C, (△) at −40°C

* *Errata:* The coefficient β was incorrectly printed as 1/2 in ref. 3.

It is interesting to note that the extrapolated values for τ_0 are the same for compression as for tension, both at $-40°C$ and at $-25°C$. Thus in the more general equation introduced previously[9], derived from the time-lag analysis of Frisch[12,13]:

$$\tau(\lambda,T)=a\exp\left(\frac{bT_m^2}{T(T_m-T)^2}+\frac{c}{d+T-T_g}+\beta\lambda\right) \quad (4)$$

the same values for the constants apply for crystallization in compression, with the single exception of a sign change for β. Thus, $a=9.5\times10^{-2}$, $b=12.3$, $c=247$, $d=22.5$ and $T_m=30°C$. The relationship between temperature and nucleation period thus appears unaffected by the mode of deformation.

Effects of crystal growth. In spite of the large variation in initial compression moduli, the growth phase of crystallization was adequately described by an Avrami function of the form:

$$\frac{E(\infty)-E(t)}{E(\infty)-E(0)}=\exp[-Kt^n] \quad (5)$$

where $E(\infty)$ is the incremental compression modulus of equation (1) at equilibrium, and $E(t)$ and $E(0)$ represent the modulus at times t and zero respectively. As before[9], n is the Avrami coefficient and K the Avrami constant.

Figure 4 illustrates the conformity to equation (5) in that the expected linear plots were obtained. The solid lines in *Figure 2* were obtained theoretically from equation (5) using empirically determined values for n and K.

In uniaxial compression, the compression ratio λ_c is less than 1, and is defined by:

$$\lambda_c=1-e_c \quad (6)$$

where e_c is the axial compression strain.

If the principal extension ratios along three mutually perpendicular axes are represented by λ_1, λ_2 and λ_3, then if the volume of rubber remains constant:

$$\lambda_1\lambda_2\lambda_3=1 \quad (7)$$

Equation (7) is a reasonable approximation for the shape of rubber discs used in the experiments, prior to

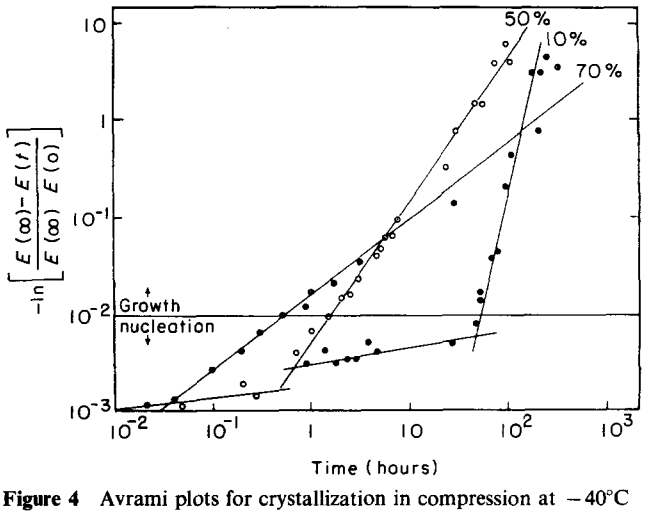

Figure 4 Avrami plots for crystallization in compression at $-40°C$

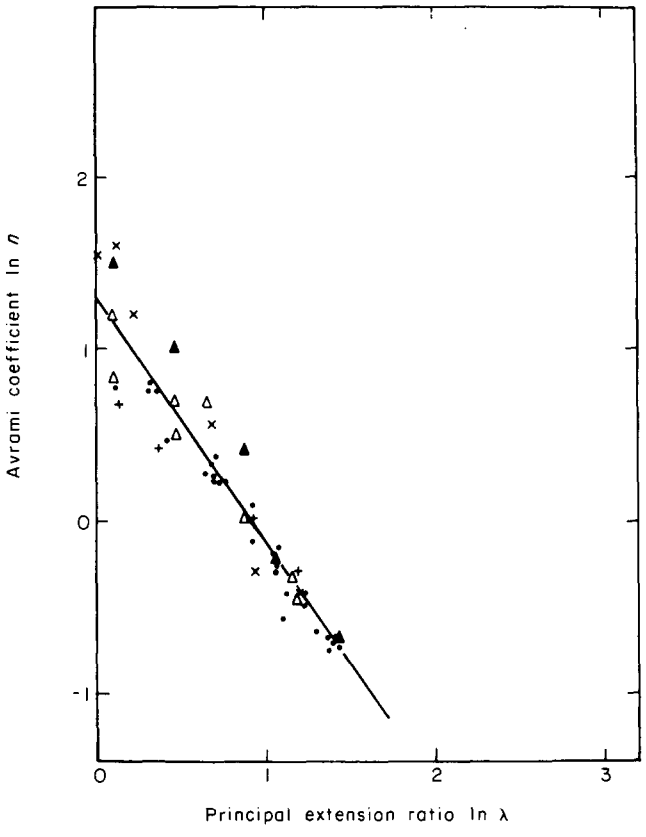

Figure 5 Avrami coefficient $\ln n$ vs. principal extension ratio $\ln n$ (or λ_c^{-1}) symbols as per *Figure 3*

crystallization. The extension of lateral dimensions corresponding to a uniaxial compression ratio λ_c is thus

$$\lambda_3=\lambda_2=\lambda_c^{-1/2} \quad (8)$$

However, the crystallization behaviour did *not* scale with this parameter but instead with λ_3^2 (i.e. λ_c^{-1}). Thus in *Figure 5* when the Avrami coefficient n is plotted against λ_c^{-1}, the data coincides exactly, within experimental error, with data obtained with tensile strains, where $\ln n$ was plotted against λ. It is interesting that a common plot can be obtained for these two different modes of deformation which uniquely characterizes the growth phase of crystallization.

Equilibrium modulus. Equilibrium values of compression modulus were attained after long time periods when the 'final' semi-crystalline state was reached. Unlike the equilibrium tensile moduli[9], these compression moduli were found to depend on the strain at which crystallization occurred. In fact the strain dependence can be related to the shape factor effect described by equation (2). This is illustrated in *Figure 6*. As the test piece is compressed, there is a change of shape, which, for strains above 40% results in contact between the outer bulging rubber and the compression platens. This shape change may be considered in terms of a change in shape factor S. Before crystallization the compression modulus (as defined by equation (1)) increased strongly with applied strain, e_c, or equivalent shape factor S. It is interesting that this shape dependence persists *after* crystallization, even though actual moduli are all increased by a factor of 100. A fully crystalline material would not be expected to exhibit shape factor dependence and this is further

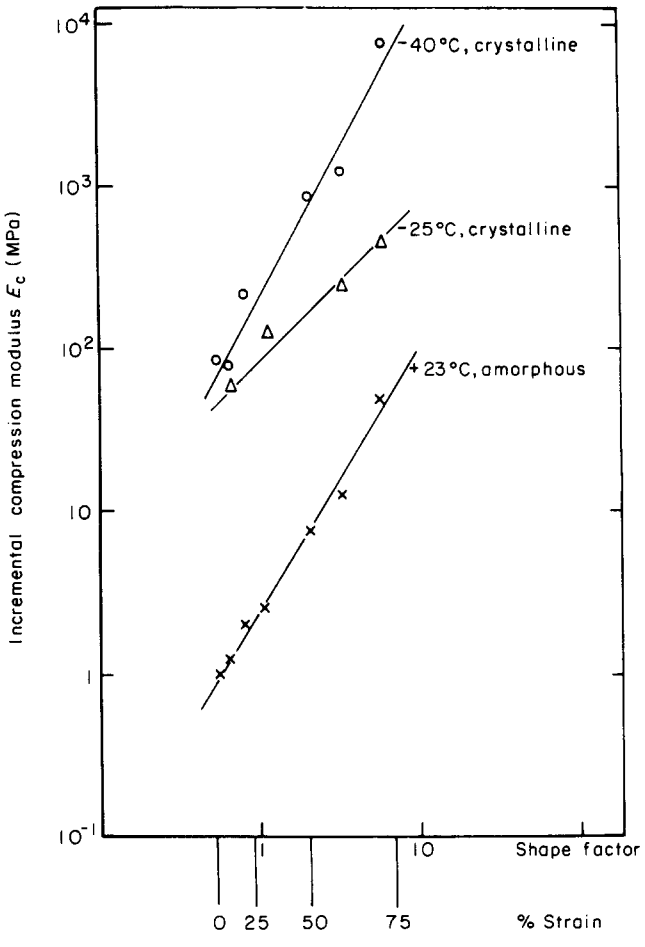

Figure 6 Effect of shape factor on compression modulus (a) crystalline, (b) amorphous

evidence that NR only ever becomes partially crystalline (*circa* 30%) and that its modulus is still strongly influenced by deformations in the amorphous phase, constrained by the crystalline phase—rather than by deformation of crystalline rubber. At very high strains however (> 70%) and low temperatures (< −40°C) there may be some evidence that the crystalline phase is itself constrained to deform—resulting in an even higher modulus.

Morphology. The morphology of crystallization under uniaxial compression cannot be studied directly by the use of thin film transmission electron microscopy due to the three dimensional nature of the strain field. Freeze-fractured surfaces from bulk specimens were therefore studied for any correlations with the modulus change measurements. After crystallization in compression for several months, some test pieces were immersed in liquid nitrogen, while still semi-crystalline, and fractured. The resulting fracture surfaces were then studied with a scanning electron microscope at room temperature. Since melting of the crystalline phase will occur at room temperature this technique is indirect and will only reveal where fracture paths were strongly influenced by the crystallinity. A typical 'freeze-fracture' surface of an amorphous control sample is shown in *Figure 7*. There are wavelike markings of generally irregular orientation. However for semi-crystalline compression test pieces, the fracture markings at the outer edges (see *Figure 8a*) were oriented to reflect lines that would have been lines of principal strain when the sample was in the compressed state. This orientation is illustrated in *Figure 9*, schematically. Any lines of orientation in the compressed, semi-crystalline state become inverted on heating to room temperature. More dramatic are the markings at the centre of the test piece where crystallization occurred in rubber subjected to (hydrostatic) compression without bulging and where planes are likely to have remained plane after melting (from heating to room temperature for SEM study). In this region only, a series of cleavage steps (*Figure 8b*) and finer near parallel lines (*Figure 8c*) were observed; suggesting a structure of flat platelets. It is possible for crystallization to have taken this form in this region. The planes shown in *Figure 8b* were approximately parallel to the outer loaded surfaces. These observations do thus suggest a correlation between morphology and force/deflection behaviour.

Crystallization in shear

Deformation in shear creates a simpler strain distribution field than does deformation in compression. The quadruple shear test pieces illustrated in *Figure 1* essentially produce simple shear in each of the four rubber blocks. The shear modulus, G, is then related to the Young modulus by the following approximate relation:

$$G = E_0/3 \tag{9}$$

In a simple shear, the shear strain e_s may be related to the angle of deformation θ or to the principal extension ratios λ by:

$$e_s = \tan\theta = \lambda - 1/\lambda \tag{10}$$

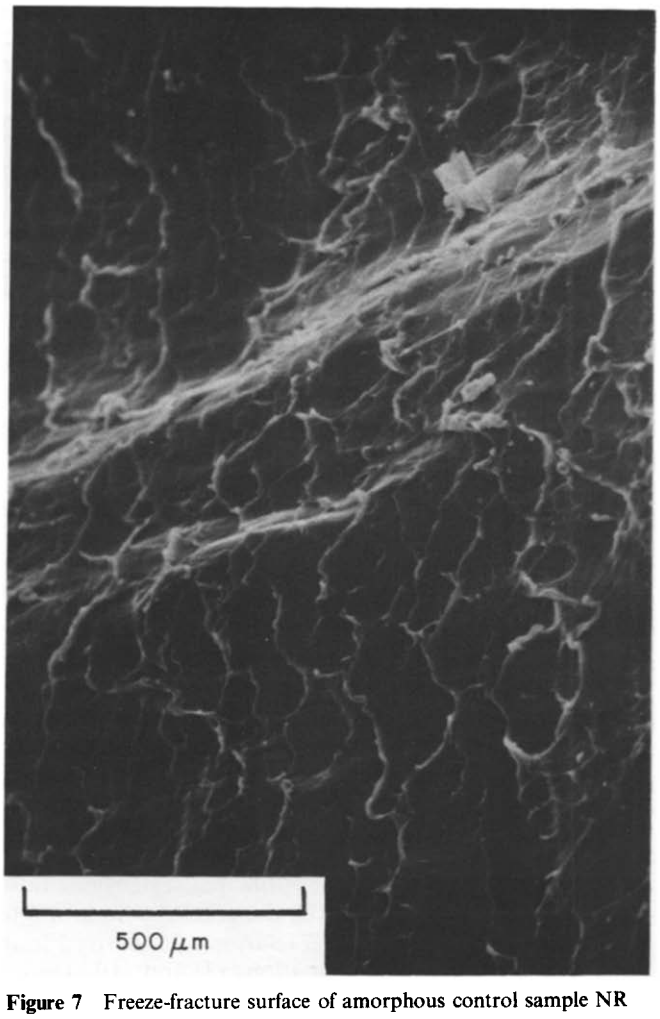

Figure 7 Freeze-fracture surface of amorphous control sample NR

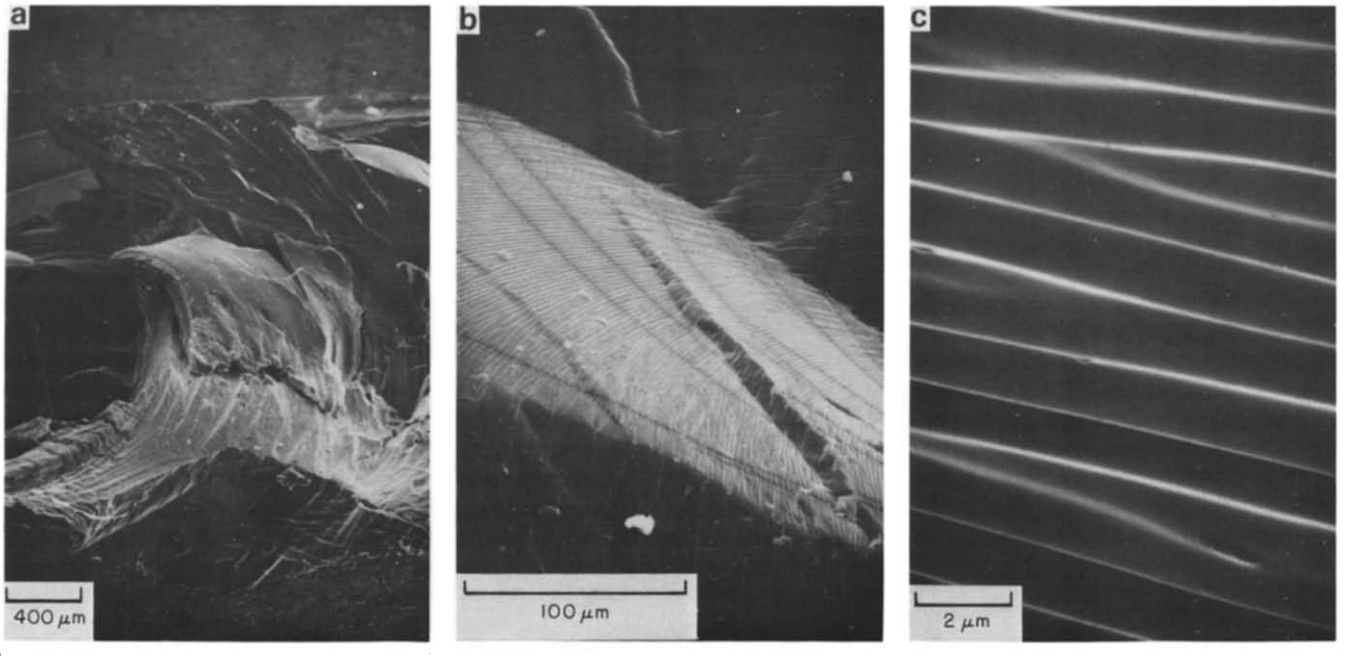

Figure 8 (a) Fracture surface markings near outer edge of compression test piece. (b) Fracture surface markings for central region, crystallized under hydrostatic compression. (c) Magnified view of central planes of 'platelets'

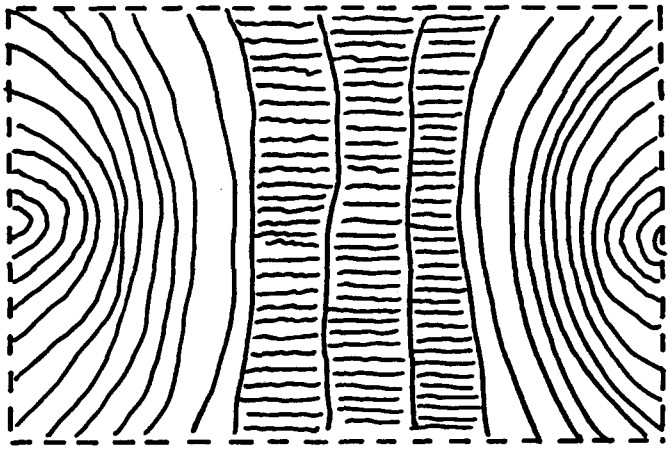

Figure 9 Schematic view of fracture marking orientations for crystalline test piece compressed to 40% at −40°C

where $\lambda_1 = \lambda, \quad \lambda_2 = 1, \quad \lambda_3 = 1/\lambda$

and $G = \sigma_s/e_s$, where σ_s is shear stress

Hooke's law is a better approximation for the deformation of rubber in shear than in either compression or extension. The principal extension ratio can be calculated from equation (10) for any applied shear deformation.

The low temperature modulus increases for shear were similar to that described previously. *Figure 10* illustrates a typical set of results, showing the effect of crystallization at −40°C with constant shear strains between 20% and 400%. Increasing the shear pre-strain decreased the induction period τ, as for compression and tension. When τ was plotted against the principal extension ratio calculated from equation (10), the results were found to agree quantitatively with the relation $\tau_0 e^{\beta\lambda}$ derived from the other two cases (see equations (3) and (4)). Thus a single unique relation describes the effect of strain on induction period that does not depend on the mode of deformation but only on the magnitude of the principal strain. This is illustrated in *Figure 3*.

The growth of the crystalline phase was again successfully described by means of Avrami functions of the form of equation (5). Plots were constructed similar to *Figure 4*, from the linear portions of which the Avrami coefficients n were determined. These were plotted against the principal strain λ, with the result (see *Figure 5*), that a single relationship defined the behaviour in all modes of deformation. Thus it is the magnitude of the strain in the rubber rather than any directional effects that appears entirely to control the nucleation and growth of the crystalline phase. In defining the Avrami plots the highest measured value after three months' exposure to the test temperature was used for $E(\infty)$. In most cases, this is clearly at least a quasi-equilibrium value—however at the highest strains there was no clear approach to equilibrium and so the values used for $E(\infty)$ must be treated with some caution.

At equilibrium, there was a distinct difference between the behaviour in shear and in compression. In shear, there was no shape factor effect and consequently no great difference between the equilibrium moduli at different strains. Indeed, the evidence suggests that the equilibrium shear modulus at high strains may be lower than at low strains—the reverse of the situation in compression. The very slow approach to equilibrium at high strains may however eventually produce equal 'equilibrium' shear moduli. Even longer experiments would be required to be definitive on this point.

DISCUSSION AND CONCLUSIONS

The growth of a crystalline phase in amorphous natural rubber at low temperatures causes an increase in Young modulus of up to two orders of magnitude. This occurs whether or not there is prior strain orientation in the amorphous phase. Indeed the presence of such prior

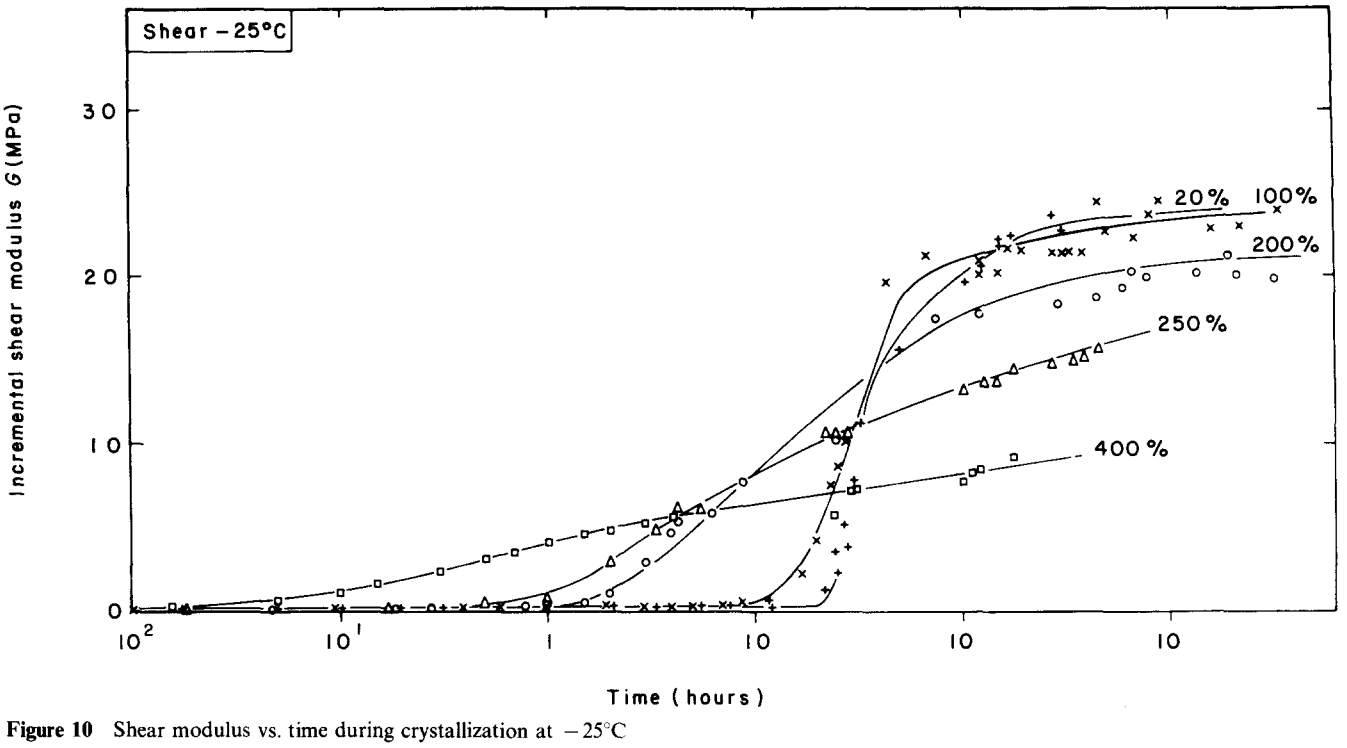

Figure 10 Shear modulus vs. time during crystallization at −25°C

strain orientation accelerates the crystallization process for all modes of deformation (shear, compression and tension). This result is consistent with most previously published work[7,9,16], but clearly refutes the claim of Reed[15] that '...the modulus of oriented amorphous material is always slightly greater than that of semi-crystalline material when $\lambda > 2.4$'. The conclusion from the work presented here is that the introduction of a crystalline phase causes a modulus increase which is at least an order of magnitude greater than that caused by strain orientation alone. Indeed, the modulus increase at high strains at room temperature are at least in part attributable to the growth of a crystalline phase. The presence of a crystalline phase has been shown[17] (by wide-angle X-ray scattering) to exist in natural rubber at high extensions even at elevated temperatures.

Different modes of deformation (compression, shear and tension) are likely to be associated with different morphological structures (fibrules, lamellae, platelets, etc.). In spite of this, the effect of pre-strain on the crystallization kinetics was similar for each mode of deformation. It proved possible to define a unique strain parameter (e.g. principal strain) in terms of which the strain dependence of the crystallization kinetics was successfully described by a common empirical relation for all modes of deformation. This result suggests that the crystallization kinetics, at least when characterized by macroscopic modulus measurements, are independent of morphology at that level.

In all cases there was a well defined time lag before any significant modulus increase. This time lag decreased with increasing pre-strain according to an empirical relation which was the same for all modes of deformation. This behaviour is consistent with the view[17] that crystallization involves growth from very small but well aligned nuclei. Increasing the test piece pre-strain will increase the initial orientation in the amorphous phase. The nuclei may themselves be aligned molecular chain segments which include some discontinuity, such as an entanglement.

At very high pre-strains nuclei for low temperature crystallization will be provided by strain induced crystallization. There is evidence[6,9] that nuclei that can persist after melting would normally be thought complete, complicating the otherwise apparent reversibility of the crystallization process.

The end of the nucleation phase was defined by a modulus change approximately equivalent to the growth of 0.3% crystallinity (assuming 30% at equilibrium). Subsequent growth of the crystalline phase was adequately described in each case by the Avrami kinetic functions. The Avrami coefficient decreased with increasing pre-strain (i.e. λ) in accordance with the same empirical relation for all temperatures and modes of deformation. Thus:

$$n = \lambda^p \exp(q) \qquad (11)$$

where $p = -1.4$ and $q = 1.3$. These values for p and q are the same as found previously for the crystallization of this rubber in tension[9]. The data is thus consistent with the view that there is a single relationship between pre-strain and growth rate coefficient for all temperatures and all modes of pre-strain.

There were however differences between the effect of different temperatures and different modes of pre-strain on the final modulus at the equilibrium state of partial crystallinity. In general, the amount of pre-strain seemed not to strongly affect the final modulus. The exception to this was compression, where the shape dependence which is well known for amorphous rubber[11] appears to persist in the semi-crystalline state. The scale of the modulus increase (exceeding a factor of 100) is generally consistent with the crystalline phase acting as a loosely woven fabric reinforcement. Indeed, composite theory has been suggested[16] as an approach to calculating increases in

modulus caused by polymer crystallization. In compression, the modulus increase was consistent witn crystallized platelets acting as reinforcing layers parallel to the loaded surfaces. This indeed correlates with the (indirect) observation of a platelet structure on freeze fractured compression test pieces examined by scanning electron microscopy. The size of these features is too great (100 mm) to be individual crystal thicknesses, but they may be caused by higher level arrangements of numbers of crystals.

The growth of a crystalline phase has been shown[17] to substantially enhance molecular orientation in the remaining amorphous phase. This enhanced orientation, combined with some inter-connection of crystalline material seems the most likely explanation for the very large modulus increases observed. Interaction between crystalline and oriented but amorphous rubber may also provide an explanation for the relatively small degree of crystallinity at equilibrium (*circa* 30%). Crystalline growth only occurs with some molecular chain movements which increase the orientation and stored elastic energy in the amorphous phase until this is high enough to prevent further crystallization. According to this mechanism, it is also possible that the different pre-strains and temperatures discussed actually cause different degrees of crystallinity.

Crystallization from rapidly strained melts, strained gels and strained solutions in which there is considerable molecular extension, is generally considered to occur with a 'chain extended type' morphology. At high pre-strains, the crystallization of lightly crosslinked NR may be similar and may already contain a substantial 'chain extended morphology' due to the pre-strain at 22°C. Subsequent low temperature crystallization (e.g. at −25°C) will then proceed from these pre-existing crystals as nuclei, leading to a possibly complex final morphology. The complexity would not be eliminated by pre-straining after equilibriating at −25°C since crystal nuclei would then initiate at zero strain but grow at a different pre-strain with a possibly different morphological type. Specimens crystallized at low temperature without sufficient pre-strain to cause extensive crystallization at 22°C may exhibit a different morphology, of lamellar crystals of the 'chain folded' type. Such crystals would be expected to be arranged in an essentially spherulitic configuration. In general, and especially in a specimen pre-strained in shear or compression, there is likely to be a mixture of morphological types—which is likely to affect the equilibrium value of the modulus. This may explain the differences observed in apparent equilibrium modulus with different shear pre-strains (*Figure 10*).

It should be emphasized again that the aim of this study was to investigate the kinetics of crystallization in rubber by means of modulus change measurements. This is a macroscopic approach which provides no direct evidence for morphological structure. Some consequences of the results for possible physical mechanisms have, however, been discussed. The resulting empirical equations describing the effect of pre-strain on low temperature crystallization kinetics may be of practical assistance in understanding and predicting the behaviour of rubber in engineering components subjected to low environmental temperatures. The processes described may also provide a model for some aspects of crystallization in other polymers.

ACKNOWLEDGEMENTS

The author would like to thank the Board of the Malaysian Rubber Producers' Research Association for permission to publish this paper and J. Lee and I. Gregory for assistance with the experiments.

REFERENCES

1 Keller, A., Hill, M. and Barham, P. *Colloid Polym. Sci.* 1980, **258**, 1023
2 Kuo, C. C. and Woodward, A. E. *Macromolecules* 1984, **17**, 1034
3 Martuscelli, E., Riva, F., Selliti, C. and Silvestre, C. *Polymer* 1985, **26**, 270
4 Andrews, E. H. *Proc. Roy. Soc., London A* 1964, **277**, 562
5 Bekkedahl, N. and Wood, L. *Ind. Eng. Chem.* 1941, **33**, 381
6 Gent, A. N. *Trans. Faraday Soc.* 1954, **50**, 521
7 Leitner, M. *Trans. Faraday Soc.* 1955, **51**, 1015
8 Stevenson, A. *Kautsch. Gummi Kunstoffe* 1984, **37**, 105
9 Stevenson, A. *J. Polym. Sci., Polym. Phys. Edn.* 1983, **21**, 553
10 Avrami, M. *J. Chem. Phys.* 1941, **9**, 177
11 Gent, A. N. and Lindley, P. B. *Proc. Inst. Mech. Eng.* 1959, **173**, 111
12 Frisch, H. L. *J. Chem. Phys.* 1957, **27**, 90
13 Frisch, H. L. and Carlier, C. C. *J. Chem. Phys.* 1971, **54**, 4326
14 Love, A. E. H. 'The Mathematical Theory of Elasticity', Cambridge University Press, 1934
15 Reed, P. E. *Proc. Roy. Soc. London A* 1974, **338**, 459
16 Halpin, J. C. and Kardos, J. L. *J. Appl. Phys.* 1972, **43**, 2235
17 Mitchell, G. R. *Polymer* 1984, **25**, 1562